

CHARACTERISATION OF ANTI-ARRHYTHMIC DRUG EFFECTS ON CARDIAC ELECTROPHYSIOLOGY USING PHYSICS-INFORMED NEURAL NETWORKS

Ching-En Chiu¹ Arieh Levy Pinto* Rasheda A Chowdhury² Kim Christensen³ Marta Varela²

¹ Department of Electrical and Electronic Engineering, Imperial College London, United Kingdom

² National Heart and Lung Institute, Imperial College London, London, United Kingdom

³ Blackett Laboratory, Imperial College London, London, United Kingdom

ABSTRACT

The ability to accurately infer cardiac electrophysiological (EP) properties is key to improving arrhythmia diagnosis and treatment. In this work, we developed a physics-informed neural networks (PINNs) framework to predict how different myocardial EP parameters are modulated by anti-arrhythmic drugs. Using *in vitro* optical mapping images and the 3-channel Fenton-Karma model, we estimated the changes in ionic channel conductance caused by these drugs.

Our framework successfully characterised the action of drugs HMR1556, nifedipine and lidocaine – respectively, blockade of I_K , I_{Ca} , and I_{Na} currents – by estimating that they decreased the respective channel conductance by $31.8 \pm 2.7\%$ ($p = 8.2 \times 10^{-5}$), $80.9 \pm 21.6\%$ ($p = 0.02$), and $8.6 \pm 0.5\%$ ($p = 0.03$), leaving the conductance of other channels unchanged. For carbenoxolone, whose main action is the blockade of intercellular gap junctions, PINNs also successfully predicted no significant changes ($p > 0.09$) in all ionic conductances.

Our results are an important step towards the deployment of PINNs for model parameter estimation from experimental data, bringing this framework closer to clinical or laboratory images analysis and for the personalisation of mathematical models.

Index Terms— Cardiac Electrophysiology, Physics-Informed Neural Networks (PINNs), Parameter Identification, Optical Mapping, Mathematical Modelling

1. INTRODUCTION

Physics-Informed Neural Networks (PINNs) are a machine learning method that combines knowledge of the equations of a system with data learning [1]. This domain knowledge allows PINNs to learn from a small fraction of the data that conventional neural networks require and ensures predictions consistent with physics models. This makes PINNs a suitable candidate for biomedical applications, where data are often sparse and noisy and interpretability is highly desired.

*The second author performed the work while at Department of Biomedical Engineering, Imperial College London, London, United Kingdom.

Within cardiac EP, Sahli-Costabal *et al.* used PINNs to solve the isotropic diffusion eikonal equation, using *in silico* data. They estimated arrival times of the action potential (AP) and conduction velocity maps across the left atrial surface [2]. Following this work, Grandits *et al.* solved the anisotropic eikonal equation to learn fibre orientations and conductivity tensors, using synthetic data and data from one patient [3]. Closely related to our work, Herrero Martin *et al.* used PINNs with the monodomain equation on sparse maps of transmembrane potential to estimate EP parameters, such as the isotropic diffusion coefficient or surrogates of the AP duration [4]. The study relied on the Aliev Panfilov model, a simple 2-variable model without clear biological counterparts [5]. To provide clinically useful characterisation of cardiac EP properties under the influence of drugs, PINNs will need to be deployed in EP models that better capture ionic channel complexity and demonstrate its ability to make inferences from experimental data.

To this end, we coupled PINNs with the Fenton-Karma model, which is a 3-variable model of the cardiac AP with formulations of three transmembrane currents: a fast inward I_{fi} , slow outward I_{so} , and slow inward I_{si} [6]. They are analogous to Na^+ , K^+ , and Ca^{2+} currents, respectively. We selected this model for its ability to reproduce restitution properties and capture arrhythmic conditions, with the appropriate level of complexity for PINNs. The Fenton-Karma equations are as follows:

$$\partial_t u = \nabla \cdot (D \nabla u) - J_{fi}(u; v) - J_{so}(u) - J_{si}(u; w), \quad (1a)$$

$$\partial_t v = \Theta(u_c - u)(1 - v)/\tau_v^- (u) - \Theta(u - u_c)v/\tau_v^+, \quad (1b)$$

$$\partial_t w = \Theta(u_c - u)(1 - w)/\tau_w^- - \Theta(u - u_c)w/\tau_w^+, \quad (1c)$$

where the three scaled currents are given by

$$J_{fi}(u, v) = -\frac{v}{\tau_d} \Theta(u - u_c)(1 - u)(u - u_c), \quad (2a)$$

$$J_{so}(u) = \frac{u}{\tau_o} \Theta(u_c - u) + \frac{1}{\tau_r} \Theta(u - u_c), \quad (2b)$$

$$J_{si}(u; w) = -\frac{w}{2\tau_{si}} (1 + \tanh[k(u - u_c^si)]). \quad (2c)$$

Here, u is the dimensionless electrical potential across the cell membrane, scaled to take values from 0 to 1. v and w are the latent gate variables for I_{fi} and I_{si} , respectively. $\Theta(x)$ is the Heaviside step function defined by $\Theta(x) = 1$ for $x \geq 0$ and $\Theta(x) = 0$ for $x < 0$. Membrane potential diffuses to the neighbouring cells, as modelled by the diffusion term for u , $\nabla(D\nabla u)$. We assume homogeneous and isotropic conduction, in which case D is a constant scalar. The 8 τ parameters are various time constants. Among them, τ_d , τ_r , τ_o , and τ_{si} are inversely proportional to ionic channel conductances, as shown in Eq. (2a)-(2c). We model the effects of anti-arrhythmic drugs as time-independent reductions in channel conductances, that is, as increases in the τ variables.

Aims. We aim to demonstrate how PINNs can characterise the effects of anti-arrhythmic drugs on ionic channels using *in vitro* optical mappings images from cardiomyocyte preparations. We will use PINNs to solve the Fenton-Karma equations and simultaneously estimate model parameters related to ionic channel conductances. For this we will use:

1. *in silico* data, which allow us to assess the accuracy and tune the model.
2. *in vitro* optical mapping data from cardiomyocyte preparations.

2. METHODS

All code used in this study is available at github.com/annien094/EP-PINNs-for-drugs.

2.1. *In Silico* Data Generation

We generated *in silico* membrane potentials on a 1D cable of 10mm by solving the Fenton-Karma model with a central finite difference and an explicit 4-stage Runge-Kutta method, using a time step of $5\mu\text{s}$ and a spatial step of $100\mu\text{m}$. The values of model parameters were set as in [7] (see FK-CAF model). We used APs across time from two spatial points as inputs to the PINNs, to mimic the available experimental data. We assessed the accuracy of parameter estimation using the relative error (RE).

2.2. Optical Mapping Images

We tested the performance of our PINNs setup on *in vitro* optical mapping images from neonatal rat ventricular myocyte preparations. These preparations were stained with a voltage-sensitive dye (di-8-ANNEPS) before imaging at a high spatio-temporal resolution of 400×85 pixels at 525.39 frames/sec to obtain uncalibrated measurements of electrical potentials. All experimental details are described in [8].

We investigated the effects of four drugs: HMR1556, nifedipine, lidocaine, and carbenoxolone (CBX). Their effects are summarised in Table 1. We assessed the effects of

	HMR1556	Nifedipine	Lidocaine	CBX
Site of blockade	Potassium channel (I_K)	Calcium channel (I_{Ca})	Sodium channel (I_{Na})	Intercellular gap junctions
Effects on model parameters	Increases τ_r	Increases τ_{si}	Increases τ_d	No effect on all τ
Effects on AP	Prolongs duration	Shortens duration	Prolongs upstroke	Decreases conduction velocity

Table 1. Effects of anti-arrhythmic drugs [9, 10, 11, 12].

drugs on PINNs' estimates of model parameters. We identified drug-induced significant differences using a one-tailed two-sample t -test at a significance level of 0.05.

For each drug, we used four time series of optical mapping images. Two of these series were acquired under the action of the drug at half-maximal inhibitory concentration (IC_{50}), at two different preparation locations. The other pair was acquired in the absence of drugs (baseline conditions) also at two different locations. For each time series, we improved the signal-to-noise ratio of the data by:

- spatially averaging the signal over a circular area of radius $50\mu\text{m}$ (indicated in Fig. 1);
- applying a temporal moving average filter to the signal except at the AP upstrokes;
- correcting temporal baseline drifts by subtracting each AP by the average of 10ms before each upstroke;
- overlaying and averaging all APs across time;
- and scaling each averaged AP to the $[0, 1]$ interval.

For simplicity, we modelled the cardiomyocyte preparation as a 10mm cable with the measured APs placed at positions $x_1 = 2\text{mm}$ and $x_2 = 8\text{mm}$. A diffusion coefficient of $D = 0.1 \text{ mm ms}^{-1}$ was used. These were then used as inputs for PINNs. This pipeline is illustrated in Fig. 1.

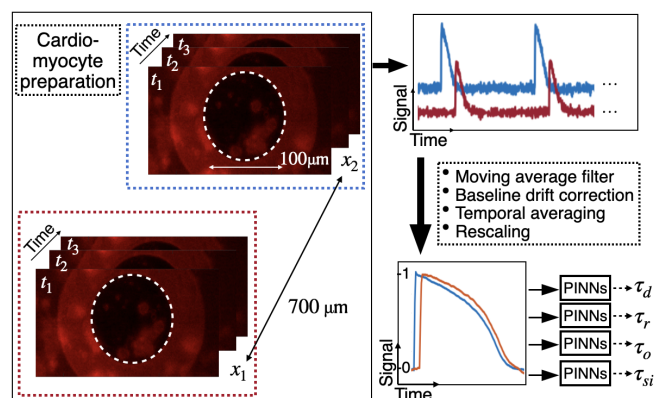


Fig. 1. Data processing pipeline for optical mapping images.

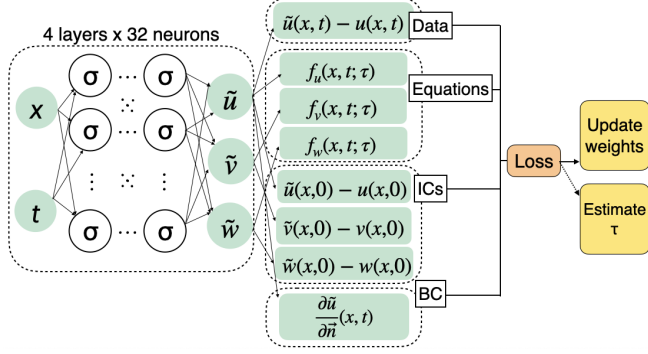


Fig. 2. The PINNs architecture. Inputs x and t are the spatial and time points. The network optimises its weights by minimising the loss function L , to provide solutions for u , v , and w . It simultaneously estimates model parameter(s) τ .

2.3. PINNs Setup

We used a fully-connected neural network with 4 layers of 32 neurons each, a \tanh activation, a Glorot Uniform initialisation, and Adam optimisation. There were two input variables, space and time position x and t , and three output variables: u , v , and w . We trained the network for 100,000 epochs with learning rate 5×10^{-5} . These hyperparameters were selected empirically based on tests using *in silico* data. The loss function consists of 8 terms:

$$L = L_{f_u} + L_{f_v} + L_{f_w} + L_{BC} + L_{IC,u} + L_{IC,v} + L_{IC,w} + L_{data}. \quad (3)$$

$L_{f_u} + L_{f_v} + L_{f_w}$ accounts for the agreement with the Fenton-Karma equations Eq. (1a)-(1c). L_{BC} and $L_{IC,u} + L_{IC,v} + L_{IC,w}$ accounts for the no-flux Neumann boundary condition for membrane voltage $\frac{\partial u}{\partial n} = 0$ and initial conditions for variables u , v , and w . L_{data} accounts for the agreement with experimental measurements of u . We empirically determined that equal weights for all terms leads to the best network performance. For training, we used 60000 points within the domain for the agreement with equations, 1000 boundary points, and 99 initial points for boundary and initial conditions. We split all available data into train and test sets at 9:1 and calculate the root mean squared error (RMSE) on the test points.

2.4. Model Parameter Estimation using PINNs

We used PINNs to estimate model parameters τ_d , τ_r , τ_o , and τ_{si} in two modes: a) individually, with the other parameters fixed at literature values (see FK-CAF in [7]), and b) estimating all four parameters simultaneously. We initialised the model parameter(s) by randomly drawing from a uniform distribution around the ground truth(s), where the distribution widths were based on uncertainties from preliminary results.

To estimate the uncertainty in parameter estimates, the network was randomly initialised to a different configuration

five times and the standard deviation of the model parameter estimates over these runs was computed.

3. RESULTS

3.1. Parameter estimation with *in silico* data

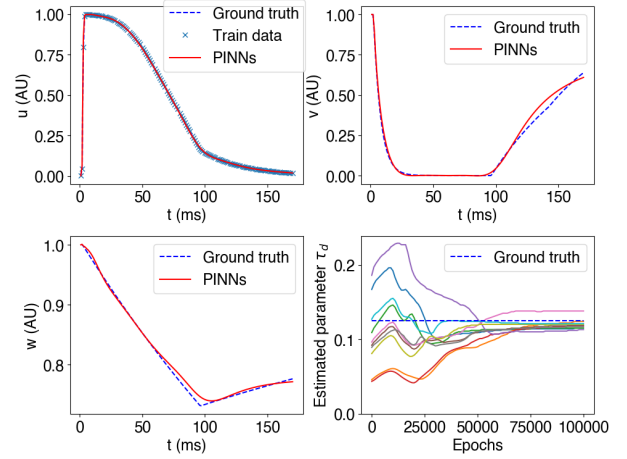


Fig. 3. PINNs' predictions and *in silico* ground truth data for transmembrane potential u and gate variables v and w at 2mm on a 1D 10mm cable. Only data for u were given here and at 8mm, and none for v and w . Bottom right: 10 independent runs of parameter estimates of τ_d across epochs.

Using PINNs, we were able to accurately estimate the Fenton-Karma model parameters, and accurately reproduce the APs and time course of latent variables, as shown in Fig. 3. PINNs predictions for variables u , v , and w are in good agreement with the synthetic ground truth data, even when only data for u were given at two locations. Estimates of the variables were not affected by the number of model parameters predicted by PINNs: RMSE was $(4.6 \pm 2.0) \times 10^{-3}$ when estimating each parameter individually, and $(4.9 \pm 2.2) \times 10^{-3}$ when estimating all four simultaneously.

As shown in Fig. 4, when estimating each parameter separately, REs were within 15%. REs were generally larger when estimating four parameters simultaneously, as expected, but even in this regime did not exceed 30%. τ_{si} (inverse of I_{Ca} conductance) was the least accurate in both modes, and τ_d (inverse of I_{Na} conductance) the most accurate.

3.2. Drug Effect characterisation using PINNs

With experimental *in vitro* data as inputs, PINNs were also able to accurately reproduce the experimental APs, with an average RMSE for u within 7×10^{-2} (Fig. 5).

Our method remarkably identified the effects of drugs on each ionic channel by measuring significant increases in the τ parameters that correspond to the ionic channels each drug

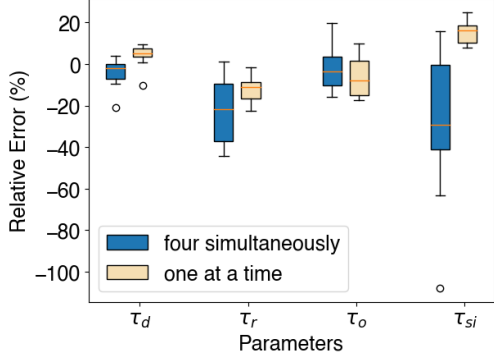


Fig. 4. Relative errors of parameter estimates using *in silico* data.

is known to modulate. The relative changes in τ and the associated p -values are reported in Table 2. We estimated each parameter separately for *in vitro* data for stability.

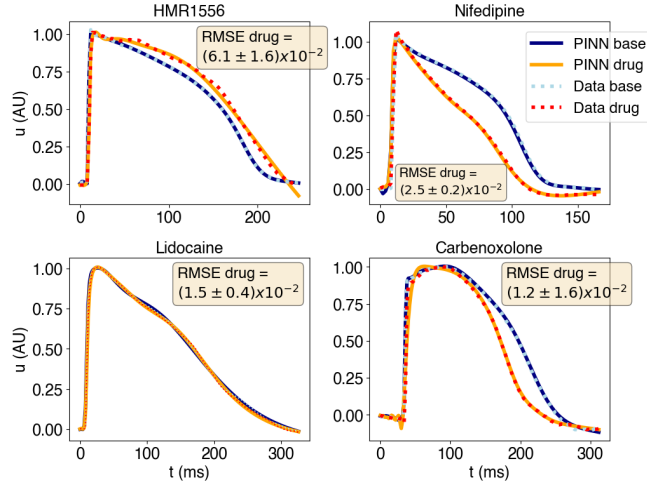


Fig. 5. PINNs’ predictions of the action potentials and *in vitro* optical mapping data showed good agreement even when some model parameters were not given to the network. The RMSE for u in baseline conditions was $(2.6 \pm 2.5) \times 10^{-2}$.

4. DISCUSSION

In this work, we developed a PINNs framework capable of accurate characterisation of anti-arrhythmic drug actions on EP parameters, using experimental *in vitro* images. We coupled PINNs with the Fenton-Karma model, which distinguishes among currents of the three main ion species in the heart: Na^+ , K^+ , and Ca^{2+} . Starting with *in silico* data, PINNs accurately estimated the model parameters corresponding to different ionic channel conductances. Then, with *in vitro* optical mapping images, PINNs identified significant increases in model parameters corresponding to the expected

	HMR1556	Nifedipine
$\Delta\tau_d$	$-3.4 \pm 0.3\%$	$-5.5 \pm 0.5\%$
p -value	0.50	0.28
$\Delta\tau_r$	$31.8 \pm 2.7\%$	$-0.69 \pm 0.04\%$
p -value	8.2×10^{-5}	0.85
$\Delta\tau_o$	$37.1 \pm 14.5\%$	$9.5 \pm 1.4\%$
p -value	0.065	0.24
$\Delta\tau_{si}$	$-13.6 \pm 2.6\%$	$80.9 \pm 21.6\%$
p -value	0.19	0.024
Expected	Increases τ_r	Increases τ_{si}

	Lidocaine	CBX
$\Delta\tau_d$	$8.6 \pm 0.5\%$	$-8.3 \pm 4.6\%$
p -value	0.03	0.73
$\Delta\tau_r$	$1.2 \pm 0.2\%$	$9.1 \pm 0.9\%$
p -value	0.84	0.09
$\Delta\tau_o$	$17.7 \pm 10.6\%$	$-8.1 \pm 6.2\%$
p -value	0.58	0.81
$\Delta\tau_{si}$	$-9.8 \pm 2.0\%$	$-2.2 \pm 0.2\%$
p -value	0.22	0.56
Expected	Increases τ_d	No change in τ

Table 2. Relative changes in the τ parameters (inverse of channel conductance) between baseline and drug and associated p -values. Significant increases in τ are shown in green.

drug-induced reduction of channel conductances. In both cases, PINNs gave excellent predictions for AP propagation, which demonstrated its capability to work well with sparse measurements, experimental noise and artefacts.

So far, studies have mostly focussed on demonstrating PINNs performance on *in silico* data [2, 13, 14]. We showed that PINNs are also effective for model calibration with *in vitro* data as inputs. Previous work had used PINNs to characterise drug effects with a simple model that does not consider ionic channels [4]. Our work shows that it is possible to use more sophisticated cardiac EP models to gain more detailed insights into drug mechanisms, which has important applications in the safety and efficacy testing of new drugs [15]. Compared to traditional numerical methods, our approach has the advantages of being mesh-free, using automatic differentiation, and can be compactly implemented to simultaneously solve forward and inverse problems [14].

Limitations in our current framework include experiment-specific results, where evaluation on other sets of data would be valuable for robustness. In addition, the parameter estimates and convergence properties are sensitive to the initialisation. Future work may focus on exploring alternative optimisation schemes and loss function compositions. We also plan to extend this framework to the analysis of electrograms to bring PINNs’ advantages closer to the clinical setting.

5. COMPLIANCE WITH ETHICAL STANDARDS

This is a computational study for which no ethical approval was required. The data used were acquired in [8], with the appropriate ethical approvals detailed therein: all procedures were conducted according to the standards set by the EU Directive 2010/63/EU and were approved by the Imperial College London Ethical Committee.

6. ACKNOWLEDGMENTS

This work was supported by the British Heart Foundation (RE/18/4/34215, RG/16/3/32175, PG/16/17/32069 and Centre of Research Excellence), the National Institute for Health Research (UK) Biomedical Research Centre and the Rose-trees Trust through the interdisciplinary award "Atrial Fibrillation: A Major Clinical Challenge".

7. REFERENCES

- [1] M. Raissi, P. Perdikaris, and G. E. Karniadakis, "Physics-informed neural networks: A deep learning framework for solving forward and inverse problems involving nonlinear partial differential equations," *Journal of Computational Physics*, vol. 378, pp. 686–707, 2019.
- [2] Francisco Sahli Costabal, Yibo Yang, Paris Perdikaris, Daniel E Hurtado, and Ellen Kuhl, "Physics-informed neural networks for cardiac activation mapping," *Frontiers in Physics*, vol. 8, pp. 42, 2020.
- [3] Thomas Grandits, Simone Pezzuto, Francisco Sahli Costabal, Paris Perdikaris, Thomas Pock, Gernot Plank, and Rolf Krause, "Learning atrial fiber orientations and conductivity tensors from intracardiac maps using physics-informed neural networks," in *International Conference on Functional Imaging and Modeling of the Heart*. Springer, 2021, pp. 650–658.
- [4] Clara Herrero Martin, Alon Oved, Rasheda A Chowdhury, Elisabeth Ullmann, Nicholas S Peters, Anil A Bharath, and Marta Varela, "Ep-pinns: Cardiac electrophysiology characterisation using physics-informed neural networks," *Frontiers in Cardiovascular Medicine*, vol. 8, pp. 768419, 2022.
- [5] Rubin R Aliev and Alexander V Panfilov, "A simple two-variable model of cardiac excitation," *Chaos, Solitons & Fractals*, vol. 7, no. 3, pp. 293–301, 1996.
- [6] Flavio Fenton and Alain Karma, "Vortex dynamics in three-dimensional continuous myocardium with fiber rotation: Filament instability and fibrillation," *Chaos: An Interdisciplinary Journal of Nonlinear Science*, vol. 8, no. 1, pp. 20–47, 1998.
- [7] Amy M Goodman, Robert A Oliver, Craig S Henriquez, and Patrick D Wolf, "A membrane model of electrically remodelled atrial myocardium derived from in vivo measurements," *EP Europace*, vol. 7, no. s2, pp. S135–S145, 2005.
- [8] Rasheda A Chowdhury, Konstantinos N. Tzortzis, Emmanuel Dupont, Shaun Selvadurai, Filippo Perbellini, Chris D. Cantwell, Fu Siong Ng, Andre R. Simon, Cesare M. Terracciano, and Nicholas S. Peters, "Concurrent micro-to macro-cardiac electrophysiology in myocyte cultures and human heart slices," *Scientific Reports*, vol. 8, no. 1, pp. 1–13, 12 2018.
- [9] George P Thomas, Uwe Gerlach, and Charles Antzelevitch, "Hmr 1556, a potent and selective blocker of slowly activating delayed rectifier potassium current," *Journal of cardiovascular pharmacology*, vol. 41, no. 1, pp. 140–147, 2003.
- [10] Théophile Godfraind, "Discovery and development of calcium channel blockers," *Frontiers in pharmacology*, vol. 8, pp. 286, 2017.
- [11] BRUCE P Bean, CHARLES J Cohen, and RICHARD W Tsien, "Lidocaine block of cardiac sodium channels," *The Journal of general physiology*, vol. 81, no. 5, pp. 613, 1983.
- [12] Pipin Kojodjojo, Prapa Kanagaratnam, Oliver R Segal, Wajid Hussain, and Nicholas S Peters, "The effects of carbenoxolone on human myocardial conduction: a tool to investigate the role of gap junctional uncoupling in human arrhythmogenesis," *Journal of the American College of Cardiology*, vol. 48, no. 6, pp. 1242–1249, 2006.
- [13] Alireza Yazdani, Lu Lu, Maziar Raissi, and George Em Karniadakis, "Systems biology informed deep learning for inferring parameters and hidden dynamics," *PLoS Computational Biology*, vol. 16, no. 11, pp. 1–19, 2020.
- [14] Lu Lu, Xuhui Meng, Zhiping Mao, and G. E. Karniadakis, "DeepXDE: A deep learning library for solving differential equations," *SIAM Review*, vol. 63, no. 1, pp. 208–228, 2 2021.
- [15] Nejib Zemzemi, Miguel O Bernabeu, Javier Saiz, Jonathan Cooper, Pras Pathmanathan, Gary R Mirams, Joe Pitt-Francis, and Blanca Rodriguez, "Computational assessment of drug-induced effects on the electrocardiogram: from ion channel to body surface potentials," *British journal of pharmacology*, vol. 168, no. 3, pp. 718–733, 2013.